

# The phase diagram of QCD with four degenerate quarks

Paolo Cea

*Dipartimento di Fisica dell'Università di Bari and INFN - Sezione di Bari, I-70126 Bari, Italy\**

Leonardo Cosmai

*INFN - Sezione di Bari, I-70126 Bari, Italy†*

Massimo D'Elia

*Dipartimento di Fisica dell'Università di Genova and INFN - Sezione di Genova, I-16146 Genova, Italy‡*

Alessandro Papa

*Dipartimento di Fisica dell'Università della Calabria and INFN - Gruppo collegato di Cosenza, I-87036 Arcavacata di Rende, Cosenza, Italy§*

(Dated: July 6, 2021)

We revisit the determination of the pseudo-critical line of QCD with four degenerate quarks at non-zero temperature and baryon density by the method of analytic continuation. We determine the pseudo-critical couplings at imaginary chemical potentials by high-statistics Monte Carlo simulations and reveal deviations from the simple quadratic dependence on the chemical potential visible in earlier works on the same subject. Finally, we discuss the implications of our findings for the shape of the pseudo-critical line at real chemical potential, comparing different possible extrapolations.

PACS numbers: 11.15.Ha, 12.38.Gc, 12.38.Aw

## I. INTRODUCTION

The study of QCD at non-zero baryon density by numerical simulations on a space-time lattice is plagued by the well-known sign problem: the fermionic determinant is complex and the Monte Carlo sampling becomes unfeasible.

One of the possibilities to circumvent this problem is to perform Monte Carlo numerical simulations for imaginary values of the baryon chemical potential, where the fermionic determinant is real and the sign problem is absent, and to infer the behavior at real chemical potential by analytic continuation.

The idea of formulating a theory at imaginary  $\mu$  was first suggested in Ref. [1], while the effectiveness of the method of analytic continuation was pushed forward in Ref. [2]. Since then, the method has been extensively applied to QCD [3, 4, 5, 6, 7, 8, 9, 10] and tested in QCD-like theories free of the sign problem [11, 12, 13, 14, 15, 16, 17] and in spin models [18, 19].

The state-of-the-art is the following:

- the method is well-founded and works fine within the limitations posed by the presence of non-analyticities and by the periodicity of the theory with imaginary chemical potential [20];
- the analytic continuation of physical observables is

improved if ratios of polynomials (or Padé approximants [21]) are used as interpolating functions at imaginary chemical potential [13];

- the analytic continuation of the (pseudo-)critical line on the temperature – chemical potential plane is well-justified, but careful tests in two-color QCD [14, 17] and in three-color QCD with finite isospin density [17] have evidenced some difficulties in its application;
- also some partial information about the nature of the phase transition as a function of the chemical potential can be obtained by a careful study of the phase diagram in the  $T - \text{Im}(\mu)$  plane [7, 22, 23].

In particular, the numerical analyses in Refs. [14, 17] have shown that, while there is no doubt that an analytic function exists which interpolates numerical data for the pseudo-critical couplings for both imaginary and real  $\mu$  across  $\mu = 0$ , determining this function by an interpolation of data at imaginary  $\mu$  could be misleading. Indeed, it was found that non-linear terms in the dependence of the pseudocritical coupling  $\beta_c$  on  $\mu^2$  in general cannot be neglected and the prediction for the pseudo-critical couplings at real chemical potentials may be wrong if data at imaginary  $\mu$  are fitted according to a linear dependence. Moreover, the coefficients of the linear and non-linear terms in  $\mu^2$  in a Taylor expansion of  $\beta_c(\mu^2)$  are all negative. That often implies subtle cancellations of non-linear terms at imaginary chemical potentials ( $\mu^2 < 0$ ) in the region available for analytic continuation (first Roberge-Weiss sector). The detection of such terms, from simulations at  $\mu^2 < 0$  only, may be difficult and requires an extremely high accuracy.

\*Electronic address: paolo.cea@ba.infn.it

†Electronic address: leonardo.cosmai@ba.infn.it

‡Electronic address: massimo.delia@ge.infn.it

§Electronic address: papa@cs.infn.it

In Refs. [14, 17] it was realized that, though a polynomial of order  $\mu^6$  seems to be sufficient in all explored cases in two-color QCD and in three-color QCD at finite isospin density, an increased predictivity can be achieved by a fit with the linear term in  $\mu^2$  fixed from data at small values of  $\mu^2$  only and kept “constrained” when data at larger values of  $\mu^2$  are included. Moreover, the idea was proposed to parameterize the critical line directly in physical units in the  $T, \mu$  plane (instead than in the  $\beta, \mu$  plane), and some Ansätze were tested for such parameterization, which provided a very good description of the critical line with a reduced number of parameters and an increased predictivity.

The aim of this paper is to apply the experience acquired through the study of sign-problem-free theories to the determination of the pseudo-critical line in three-color QCD with four degenerate quarks. With respect to the well-known work of Ref. [4], we will take advantage of the use of a smaller lattice for collecting more determinations of pseudo-critical couplings at imaginary chemical potential with increased numerical accuracy and will apply on the new lattice data the fit strategies worked out in our previous studies of Refs. [14, 17].

## II. NUMERICAL RESULTS

In our numerical analysis, we consider SU(3) with  $n_f = 4$  degenerate standard staggered fermions of mass  $am = 0.05$  on a  $12^3 \times 4$  lattice. The algorithm adopted for Monte Carlo numerical simulations is the exact  $\Phi$  algorithm described in Ref. [24], properly modified for the inclusion of a finite chemical potential.

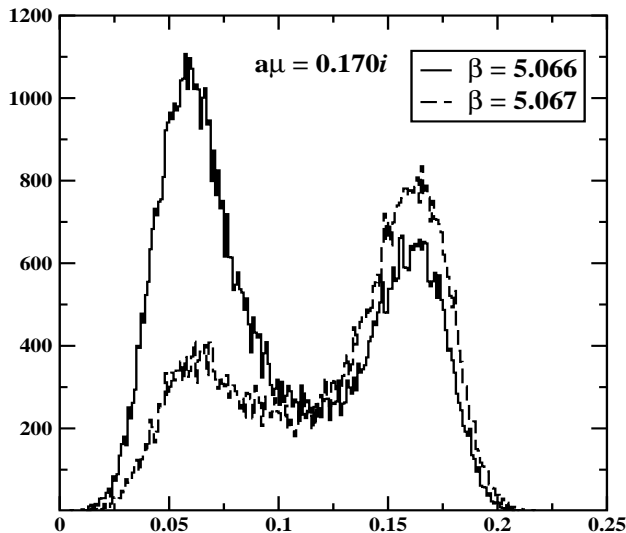


FIG. 1: Distribution of the real part of the Polyakov loop in SU(3) with  $n_f = 4$  on a  $12^3 \times 4$  lattice with  $am=0.05$  at  $a\mu = 0.170i$  and for two  $\beta$  values around the transition.

In this theory the critical line in the temperature – chemical potential plane is a line of first order transitions,

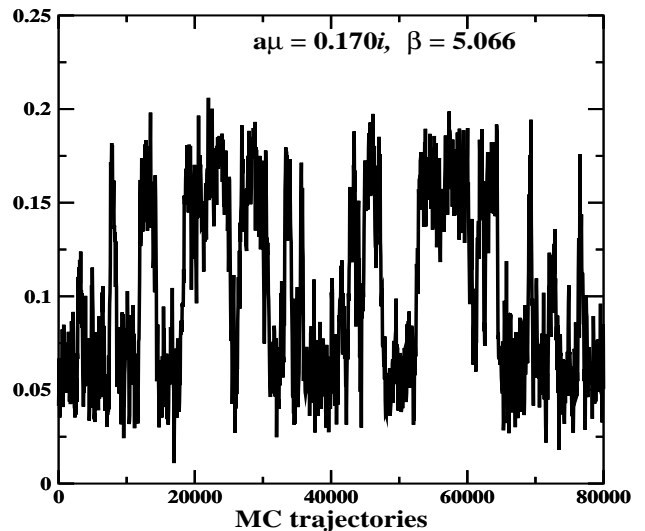


FIG. 2: Monte Carlo history of the real part of the Polyakov loop in SU(3) with  $n_f = 4$  on a  $12^3 \times 4$  lattice with  $am=0.05$  at  $a\mu = 0.170i$  and  $\beta=5.066$ .

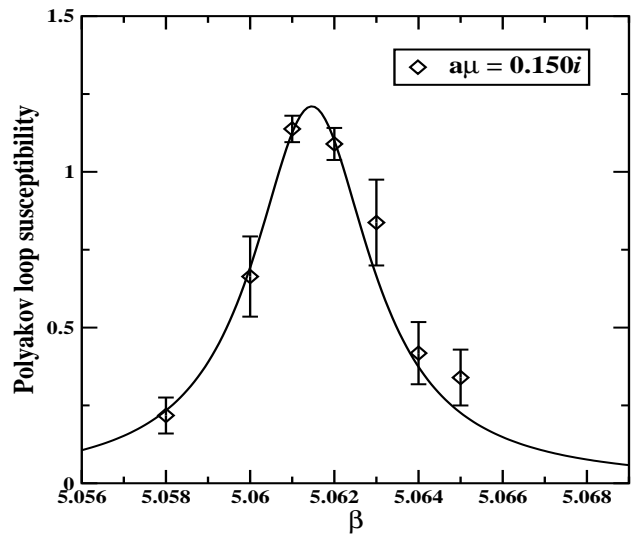


FIG. 3: Susceptibility of the (real part of the) Polyakov loop *vs*  $\beta$  in SU(3) with  $n_f = 4$  on a  $12^3 \times 4$  lattice with  $am=0.05$  and  $a\mu = 0.150i$ . The solid lines represent the Lorentzian interpolation.

over all the range of  $\mu^2$  values in the first Roberge-Weiss (RW) sector,  $-(\pi/3)^2 \leq (\mu/T)^2 \leq 0$ . Tunneling between the different phases clearly emerges from the distribution on the thermal equilibrium ensemble of the values of observables like the (real part of) the Polyakov loop, the chiral condensate, the plaquette across the transition (see Fig. 1 as an example of the typical two-peak structures). As a further evidence of the first order nature of the transition, we show in Fig. 2 the Monte Carlo run history of the (real part of) the Polyakov loop at  $a\mu = 0.170i$  and  $\beta = 5.066 \simeq \beta_c$ , which exhibits tunneling events between the two phases every few thousands trajectories, on aver-

age. Typical statistics have been around 10k trajectories of 1 Molecular Dynamics unit for each run, growing up to 100k trajectories for 4-5  $\beta$  values around  $\beta_c(\mu^2)$ , for each  $\mu^2$ , in order to correctly sample the critical behavior at the transition. The critical  $\beta(\mu^2)$  is determined as the value for which the susceptibility of the (real part of the) Polyakov loop exhibits a peak. To precisely localize the peak, a Lorentzian interpolation is used (see Fig. 3, for example). In all cases, this kind of determination is compatible with that consisting in estimating the point where the two peaks in the distribution of the (real part of the) Polyakov loop have equal height, or in locating the peak of the susceptibility by the Ferrenberg-Swendsen method. We verified also that the determinations do not change if the susceptibility of a different observable, such as the baryon number, is used. In Table I we summarize our determinations of the critical couplings: in a few cases we have repeated the determination also on a  $16^3 \times 4$  lattice, where negligible corrections, within the reported errors, have been observed. The plot of the data for  $\beta(\mu^2)$  versus  $(a\mu)^2$  – see Fig. 4 – clearly shows that data do not line up along a straight line in all the first RW sector, thus indicating that the curve  $\beta(\mu^2)$  cannot be parametrized by a polynomial of order  $\mu^2$ . In fact, as we will see soon, at least a polynomial of order  $\mu^6$  is needed to get a fit with a reasonable  $\chi^2$ .

TABLE I: Summary of the values of  $\beta_c(\mu^2)$  for SU(3) with  $n_f = 4$  on the  $12^3 \times 4$  lattice with fermionic mass  $am=0.05$ .

$a \text{Im}(\mu)$	$\beta_c$
0.	5.04259(30)
0.060	5.04550(30)
0.080	5.04839(30)
0.100	5.05121(33)
0.125	5.05590(31)
0.150	5.06150(30)
0.170	5.06647(35)
0.185	5.07136(40)
0.200	5.07664(30)
0.210	5.08031(38)
0.220	5.08419(33)
0.228	5.08668(30)
0.235	5.08961(30)
0.239	5.09243(30)
0.243	5.09407(30)
0.2465	5.09586(30)
0.250	5.09754(40)
0.2535	5.09970(42)
0.257	5.10092(31)
0.260	5.10343(30)
$\pi/12$	5.1043(5)

We have tried several kind of interpolations of the critical couplings at  $\mu^2 \leq 0$ . At first, we have considered interpolations with polynomials up to order  $\mu^6$  (see Table II for a summary of the resulting fit parameters and their uncertainties as obtained with the MINUIT minimization code). We can see that data at  $\mu^2 \leq 0$  are precise enough to be sensitive to terms beyond the order

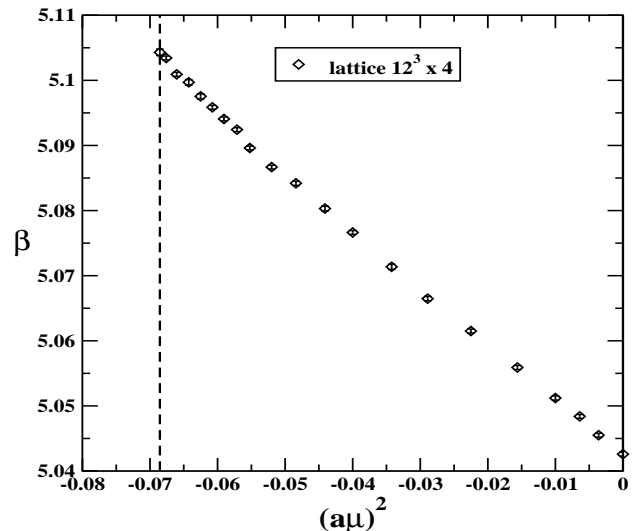


FIG. 4: Critical couplings obtained in SU(3) with  $n_f = 4$  on a  $12^3 \times 4$  lattice with  $am=0.05$ . The dashed vertical line indicates the boundary of the first RW sector,  $a \text{Im}(\mu) = \pi/12$ .

$\mu^2$ ; indeed, a good  $\chi^2/\text{d.o.f.}$  is not achieved before including terms up to the order  $\mu^6$ . In Fig. 5(left) we show how the fit with the 6th-order polynomial compares with data of  $\beta_c(\mu^2)$ ; the dotted lines around the fitting curve (solid line) delimit the 95% CL band.

As in Ref. [17], we performed a “constrained” fit: first, the largest interval  $[(a\mu)_{\min}^2, 0]$  was identified where data could be interpolated by a polynomial in  $\mu^2$ , with a  $\chi^2/\text{d.o.f.} \sim 1$ . It turned out that  $(a\mu)_{\min}^2 = (0.235i)^2$ , the quadratic coefficient being equal to  $-0.8509$ . Then, all available data were fitted by a 6th-order polynomial, with the quadratic coefficient fixed at  $-0.8509$  (see Table II and Fig. 5(right)).

Then, we have considered interpolations with ratios of polynomials of order up to  $\mu^4$  (see Table II for a summary of the resulting fit parameters). The interpolations with the least number of parameters for which we got good fits to the data at  $\mu^2 \leq 0$  are the ratio of a 2nd to 4th order polynomial and the ratio of a 4th to 2nd order polynomial (see Fig. 6(left) for the latter).

Finally, we have tried here the fit strategy first suggested in Ref. [17], consisting in writing the interpolating function in *physical units* and to deduce from it the functional dependence of  $\beta_c$  on  $\mu^2$ , after establishing a suitable correspondence between physical and lattice units. The natural, dimensionless variables of our theory are  $T/T_c(0)$ , where  $T_c(0)$  is the critical temperature at zero chemical potential, and  $\mu/T$ . The ratio  $T/T_c(0)$  is deduced from the relation  $T = 1/(N_t a(\beta))$ , where  $N_t$  is the number of lattice sites in the temporal direction and  $a(\beta)$  is the lattice spacing at a given  $\beta$ . Strictly speaking the lattice spacing depends also on the bare quark mass, which in our runs slightly changes as we change  $\beta$  since we fix  $am$ . However in the following evaluation, which is only based on the perturbative 2-loop  $\beta$ -function, we

TABLE II: Parameters of the fits to the critical couplings in SU(3) with  $n_f = 4$  on a  $12^3 \times 4$  lattice with fermionic mass  $am=0.05$ , according to the fit function  $\beta_c(\mu^2) = (a_0 + a_1(a\mu)^2 + a_2(a\mu)^4 + a_3(a\mu)^6)/(1 + a_4(a\mu)^2 + a_5(a\mu)^4)$ . Blank columns stand for terms not included in the fit. The asterisk denotes a constrained parameter. Fits are performed in the interval  $[(a\mu_{\min})^2, 0]$ ; the last column gives the value of  $(a\mu_{\min})^2$ .

$a_0$	$a_1$	$a_2$	$a_3$	$a_4$	$a_5$	$\chi^2/\text{d.o.f.}$	$(a\mu_{\min})^2$
5.04198(22)	-0.8839(48)					6.63	$-(\pi/12)^2$
5.04256(24)	-0.8509(71)					0.85	$-0.235^2$
5.04311(36)	-0.761(26)	1.77(36)				2.13	$-(\pi/12)^2$
5.04254(50)	-0.892(72)	-3.1(2.4)	-46.(23.)			1.10	$-(\pi/12)^2$
5.04277(27)	-0.8509*	-1.70(55)	-34.0(8.2)			1.20	$-(\pi/12)^2$
5.04284(28)	55.799(14)			11.2266(27)	1.741(29)	1.13	$-(\pi/12)^2$
5.04276(27)	58.196(12)	-9.46(13)		11.7044(24)		1.09	$-(\pi/12)^2$

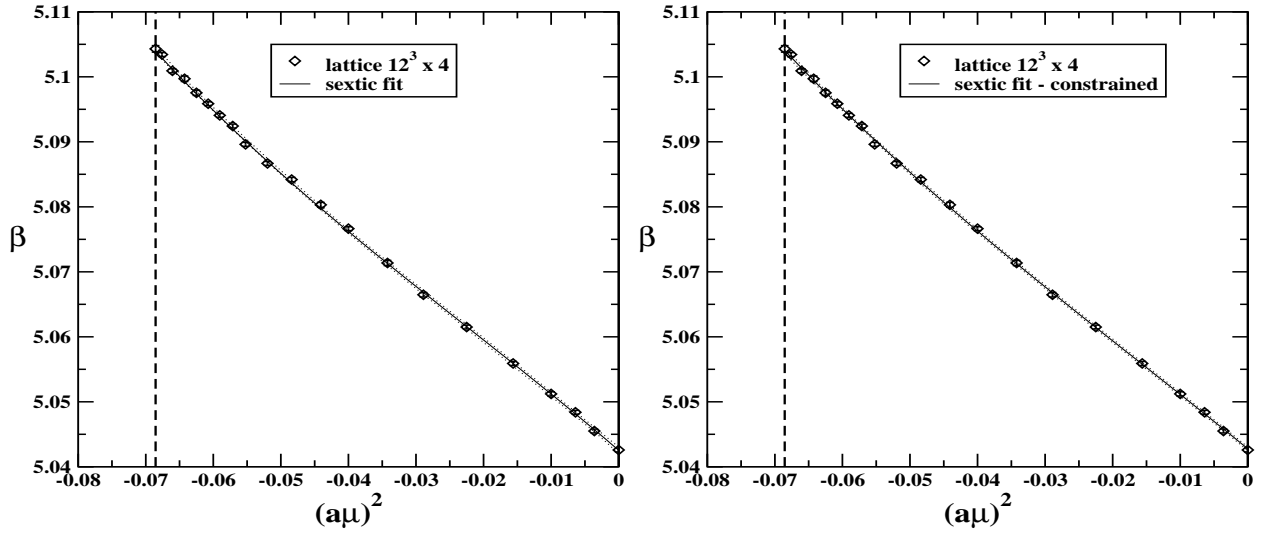


FIG. 5: Fits to the critical couplings: plain 6th order polynomial (left) and 6th-order polynomial with constrained coefficient of the quadratic term (right).

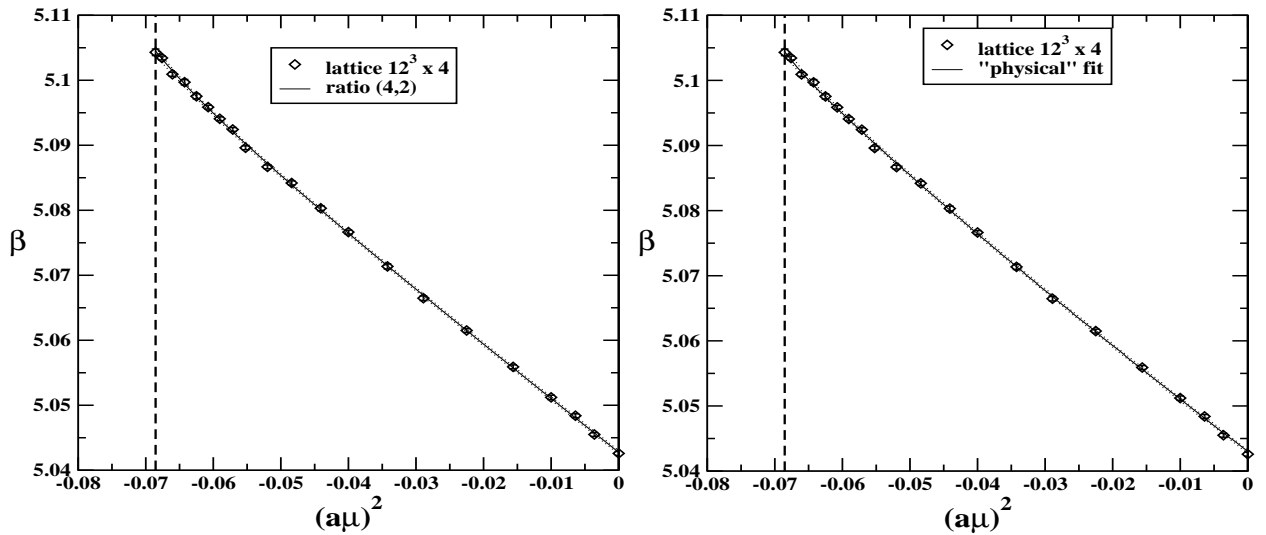


FIG. 6: Fits to the critical couplings: ratio of a 4th to 2nd order polynomial (left) and “physical” fit according to the function (2) (right).

shall neglect such dependence. We use for  $a(\beta)$  the perturbative 2-loop expression with  $N_c = 3$  and  $n_f = 4$ .

We adopted the 3-parameter function

$$\left[\frac{T_c(\mu)}{T_c(0)}\right]^2 = \frac{1 + C\mu^2/T_c^2(\mu)}{1 + A\mu^2/T_c^2(\mu) + B\mu^4/T_c^4(\mu)} \quad (1)$$

leading to the following implicit relation between  $\beta_c$  and  $\mu^2$ :

$$a^2(\beta_c(\mu^2))|_{2\text{-loop}} = a^2(\beta_c(0))|_{2\text{-loop}} \times \frac{1 + A\mu^2/T_c^2 + B\mu^4/T_c^4}{1 + C\mu^2/T_c^2}. \quad (2)$$

The values of the fit parameters turned to be

$$\begin{aligned} \beta_c(0) &= 5.04295(25), & A &= 1.00315(95), \\ B &= 0.12724(75), & C &= 0.8538(11), \end{aligned} \quad (3)$$

with  $\chi^2/\text{d.o.f.}=1.26$ . In Fig. 6(right) we compare the fit to data for  $\beta_c(\mu^2)$ .

The important question now is whether the successful interpolations we found in the  $\mu^2 \leq 0$  region have a consistent extrapolation to  $\mu^2 > 0$ . In Fig. 7 we have plotted the extrapolations to the interval  $0 \leq \mu/T \leq 2$  of the following fits:

- quadratic fit, performed in the interval  $-0.235^2 \leq (a\mu)^2 \leq 0$  (2nd line in Table II);
- sextic constrained polynomial (5th line in Table II);
- ratio (4,2) of polynomials (last line in Table II);
- “physical” fit, Eqs. (1)-(3).

The four curves agree as long as  $\mu/T \lesssim 0.6$ , but then spread. This means that different interpolations, which all reproduce the trend of data in the fit region  $-(\pi/12)^2 \leq (a\mu)^2 \leq 0$  and take correctly into account the deviation from the quadratic behavior in that region, lead to somewhat distinct extrapolations. It is evident that, unless an extra-argument is found to make one fitting function preferable with respect to the others, one cannot rely on a unique extrapolation, except in the region  $\mu/T \lesssim 0.6$ . The unpleasant aspect is that in the same region also deviations from the simple quadratic behaviour are negligible: that means that, even if we are able to see deviations from the quadratic behaviour, we are not able to extrapolate them to real chemical potentials in a reliable way, therefore the fact that we can see them is in some sense useless. That emerges as a shortcoming of analytic continuation, which however could be less severe in the more physical case of  $n_f = 2$  or  $n_f = 2 + 1$ . Indeed, in those cases, the curvature of the critical line at  $\mu = 0$  (i.e. the linear term in  $\mu^2$ ) is smaller than in the  $n_f = 4$  case and larger non-linear contributions should be needed to bend the critical line

towards a critical baryon chemical potential of the order of 1 GeV at  $T = 0$ , so that the sensitivity to such non-linear contributions could be hopefully enhanced<sup>1</sup>.

If one believes that (i) the “physical” fit has a better chance to give the correct behavior of the critical line at real chemical potential and (ii) it reproduces the critical line all the way down to  $T = 0$ , then the critical value of the chemical potential on the  $T = 0$  axis can be estimated as  $\sqrt{C/B}=2.5904(93) T_c(0)$ , yielding a critical baryon chemical potential at  $T = 0$  slightly above 1 GeV, in rough agreement with the expected lightest baryon mass. Of course neither of the two assumptions above can be supported by valid arguments.

One may ask whether a different choice of the values of the imaginary chemical potential, for which the pseudo-critical line has been located, could have improved our predictivity. Our choice in the present work has been to distribute the values more or less uniformly in  $\mu^2$ : we have then increased the density, after a preliminary analysis of our data, in the region closer to the RW transition, where deviations from the simple linear deviation in  $\mu^2$  were already visible. Of course the optimal choice could be different from that: for instance, once the region where the linear approximation works well is known, one realizes that fewer points chosen at the border of the same region would have provided the same amount of information, however this is a hint which is known only *a posteriori*.

Finally, we present in Fig. 8 an update of Fig. 4(left) of Ref. [26], where several determinations of the critical line existing in the literature are presented together with the results of this work. Looking at Fig. 8, one could comment that the extrapolation of the “physical” fit exhibits the same trend as data from reweighting, whereas that from the sextic constrained fit mimics the strong coupling behavior [27], the other two extrapolations of ours lying in-between. However, previous determinations at real  $\mu$  in the literature seem to be in fair agreement up to  $\mu/T \simeq 1.2$ . If one takes this common trend as benchmark for our extrapolations, the “physical” and the polynomial ratio (4,2) seem to be favoured.

We have tried to put the previous observation on a more solid ground, including in our fit also (subsets of) data at real chemical potential available from the literature (see Fig. 8). A serious limitation of this combined approach is the inhomogeneity of the data presently available, due to different lattices and systematics. Indeed, we could not get acceptable values of the  $\chi^2/\text{d.o.f.}$  if not restricting the region of real chemical potentials included in the fit to the interval  $0 \leq a\mu \simeq 0.6$ . Unfortunately, this is also the region where our extrapolations are consistent with each other, so that this combined fit was of little help. However, if the inhomogeneity of data at real  $\mu$

<sup>1</sup> We thank P. de Forcrand for useful comments on this point, as well as for providing us with the data needed to build up Fig. 8.

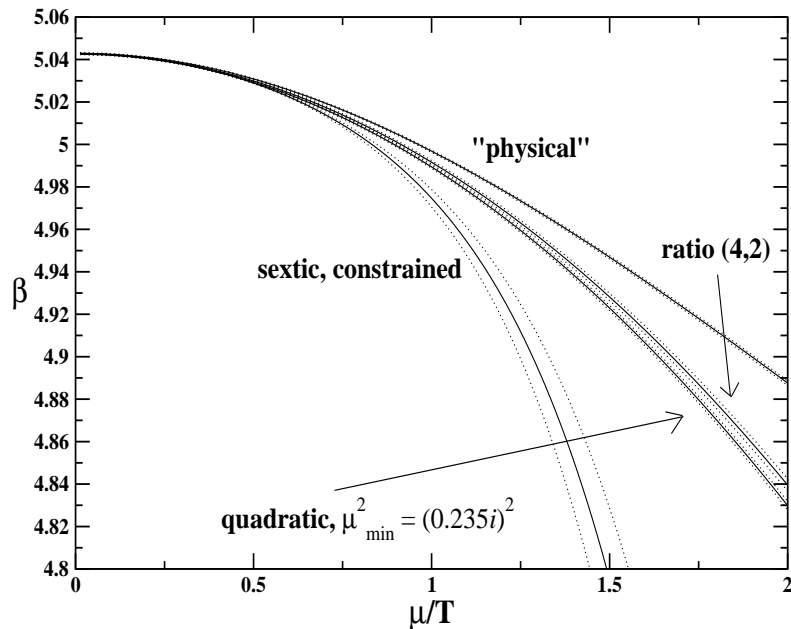


FIG. 7: Extrapolation to real chemical potentials of the quadratic (with  $(a\mu)^2 = (0.235i)^2$ ), sextic constrained, ratio of polynomials and “physical” fits.

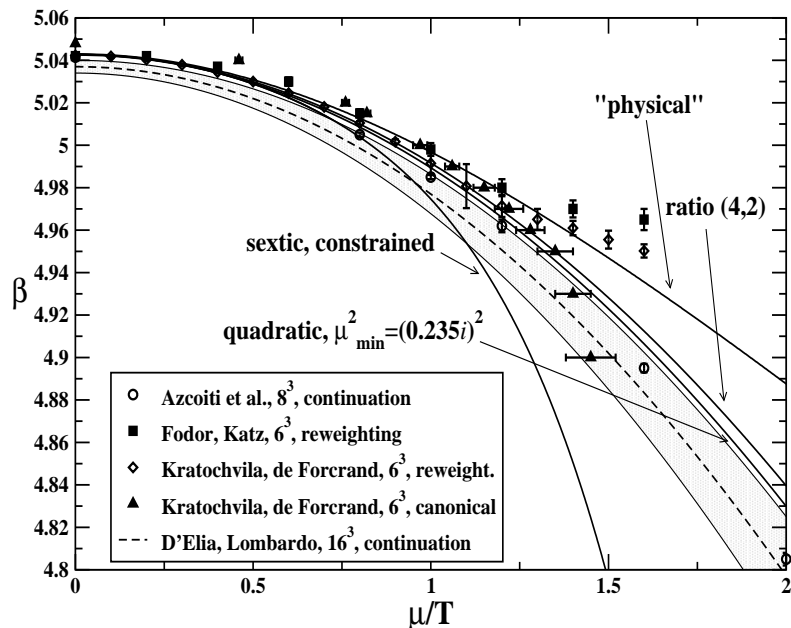


FIG. 8: Comparison of our extrapolations with other determinations in the literature. For the sake of readability, our extrapolations have been plotted without error bands and labels, since they can be easily recovered from the previous figure. *Legenda:* D’Elia, Lombardo, Ref. [4]; Azcoiti *et al.*, Ref. [5]; Fodor, Katz, Ref. [25]; Kratochvila, de Forcrand, Ref. [26].

will be reduced by new Monte Carlo determinations, the combined-fit strategy could bring along an appreciable improvement.

### III. DISCUSSION

In this paper we have revisited the application of the method of analytic continuation from imaginary to real chemical potential in QCD with  $n_f = 4$  degenerate flavors. The motivations of this study were

- to determine precisely the pseudo-critical line

$\beta_c(\mu^2)$  in the region of negative  $\mu^2$ , by sampling it through the accurate determination by Monte Carlo methods of about 20 data points, almost uniformly distributed in the region  $-(\pi/12)^2 \leq (a\mu)^2 \leq 0$  and by suitably interpolating these data points with an analytic function;

- to exploit, differently from what was hitherto done in the literature, interpolating functions sensitive to possible deviations of the critical line from the quadratic behavior in  $\mu$  for larger absolute values of  $\mu$  in the above-mentioned region; these deviations were clearly seen in QCD-like theories, such as 2-color QCD and finite isospin QCD, where it was given compelling evidence that their neglect could mislead the analytic continuation to real chemical potential;
- to extrapolate the newly adopted interpolations to the region of real  $\mu$  and to re-determine, therefore, the critical line in QCD.

The outcome has been that deviations from the quadratic behavior in  $\mu$  of the pseudo-critical couplings at negative  $\mu^2$  are indeed visible in QCD with  $n_f = 4$ . However there are several kinds of functions able to interpolate them, leading to extrapolations to real  $\mu$  which start diverging from each other for  $\mu/T \gtrsim 0.6$ . Unfortunately in the range of real chemical potentials where the different extrapolations agree, deviations from the quadratic behavior in  $\mu$  are negligible, so that our efforts to determine such deviations in the critical line in a consistent way, which were successful for QCD at finite isospin density, reveal useless in this case.

One may ask which significant differences exist between QCD at finite isospin density and QCD at finite baryon density which could be at the basis of such different outcomes. Many physical properties distinguish the two theories, but the one which is probably most

relevant to our problem is the different extension of the available region for the determination of the critical line on the imaginary chemical potential side: for QCD with an imaginary baryon chemical potential one has  $0 < \text{Im}(\mu)/T < \pi/3$ , while for QCD with an imaginary isospin chemical potential one has  $0 < \text{Im}(\mu)/T \lesssim \pi/2$  [17]. In the second case one has a wider region where more information about non-linear terms in  $\mu^2$  can be collected in order to obtain reliable extrapolations. It is indeed interesting to notice that typical deviations of  $\beta_c(\mu^2) - \beta_c(0)$  from the quadratic behaviour, visible at the border of the available region on the imaginary chemical potential side, are of the order of 5% in the present work, while they were of the order of 10% for QCD at finite isospin chemical potential.

The shortcomings of the method of analytic continuation, which emerged in this work on QCD with  $n_f = 4$ , could be less severe in the more physical case of  $n_f = 2$  or  $n_f = 2 + 1$ , where the curvature of the critical line at  $\mu = 0$  (i.e. the linear term in  $\mu^2$ ) is smaller and the sensitivity to non-linear terms in  $\mu^2$  could be enhanced. Substantial improvement could come by either theoretical developments, able to help discriminating between one kind of interpolation and another, or by combined numerical strategies, aiming at gathering information on the form of the critical line from approaches (such as reweighting, Taylor expansion, canonical approach, etc.) which have been applied so far only in exclusive way.

#### IV. ACKNOWLEDGMENTS

We are grateful to Philippe de Forcrand for useful discussions and correspondence. We acknowledge the use of the computer facilities at the INFN apeNEXT Computing Center in Rome and of the PC clusters of the INFN Bari Computer Center for Science.

- 
- [1] M.G. Alford, A. Kapustin, and F. Wilczek, Phys. Rev. D **59**, 054502 (1999).
  - [2] M.-P. Lombardo, Nucl. Phys. Proc. Suppl. **83**, 375 (2000).
  - [3] Ph. de Forcrand and O. Philipsen, Nucl. Phys. B **642**, 290 (2002); Nucl. Phys. B **673**, 170 (2003).
  - [4] M. D’Elia and M.P. Lombardo, Phys. Rev. D **67**, 014505 (2003); Phys. Rev. D **70**, 074509 (2004).
  - [5] V. Azcoiti, G. Di Carlo, A. Galante and V. Laliena, Nucl. Phys. B **723**, 77 (2005).
  - [6] H.S. Chen, X.Q. Luo, Phys. Rev. D **72**, 034504 (2005).
  - [7] Ph. de Forcrand and O. Philipsen, JHEP **0701**, 077 (2007); PoS **LATTICE2007**, 178 (2007).
  - [8] L.K. Wu, X.Q. Luo and H.S. Chen, Phys. Rev. D **76**, 034505 (2007).
  - [9] M. D’Elia, F. Di Renzo, M.P. Lombardo, Phys. Rev. D **76**, 114509 (2007).
  - [10] M. D’Elia and F. Sanfilippo, Phys. Rev. D **80**, 014502 (2009).
  - [11] A. Hart, M. Laine, and O. Philipsen, Phys. Lett. B **505**, 141 (2001).
  - [12] P. Giudice and A. Papa, Phys. Rev. D **69**, 094509 (2004); Nucl. Phys. Proc. Suppl. **140**, 529 (2005).
  - [13] P. Cea, L. Cosmai, M. D’Elia and A. Papa, JHEP **0702**, 066 (2007); PoS **LAT2006**, 143 (2006).
  - [14] P. Cea, L. Cosmai, M. D’Elia and A. Papa, Phys. Rev. D **77**, 051501 (2008); PoS **LATTICE 2007**, 214 (2007); PoS **LAT2009**, 192 (2009).
  - [15] S. Conradi, M. D’Elia, Phys. Rev. D **76**, 074501 (2007).
  - [16] Y. Shinno and H. Yoneyama, arXiv:0903.0922 [hep-lat].
  - [17] P. Cea, L. Cosmai, M. D’Elia, C. Manneschi and A. Papa, Phys. Rev. D **80**, 034501 (2009); PoS **LAT2009**, 161 (2009).
  - [18] S. Kim, P. de Forcrand, S. Kratochvila, and T. Takaishi, PoS **LAT2005**, 166 (2006).
  - [19] F. Karbstein, M. Thies, Phys. Rev. D **75**, 025003 (2007).

- [20] A. Roberge, N. Weiss, Nucl. Phys. B **275**, 734 (1986).
- [21] M.-P. Lombardo, PoS **LAT2005**, 168 (2006).
- [22] P. de Forcrand and O. Philipsen, JHEP **0811**, 012 (2008).
- [23] M. D'Elia and F. Sanfilippo, Phys. Rev. D **80**, 111501 (2009).
- [24] S. A. Gottlieb, W. Liu, D. Toussaint, R. L. Renken, and R. L. Sugar, Phys. Rev. D **35**, 2531 (1987).
- [25] Z. Fodor and S. D. Katz, Phys. Lett. B **534**, 87 (2002).
- [26] S. Kratochvila and P. de Forcrand, PoS **LAT2005** (2006) 167.
- [27] K. Miura, T. Z. Nakano, A. Ohnishi and N. Kawamoto, Phys. Rev. D **80**, 074034 (2009).